Preprints.org

Article

Not peer-reviewed version

Exploring the Application of Advanced Chromatographic Methods to Characterize the Surface Physicochemical Properties and Transition Phenomena of Polystyrene-b-Poly(4-vinylpyridine)

Tayssir Hamieh *

Posted Date: 17 September 2024

doi: 10.20944/preprints202409.1337.v1

Keywords: Adsorption; London dispersion interaction; dispersive and polar free surface energy; enthalpy and entropy of adsorption; Hamieh thermal model; glass transition; Lewis's acid-base surface energies

Preprints.org is a free multidiscipline platform providing preprint service that is dedicated to making early versions of research outputs permanently available and citable. Preprints posted at Preprints.org appear in Web of Science, Crossref, Google Scholar, Scilit, Europe PMC.

Copyright: This is an open access article distributed under the Creative Commons Attribution License which permits unrestricted use, distribution, and reproduction in any medium, provided the original work is properly cited.

Preprints.org (www.preprints.org) | NOT PEER-REVIEWED | Posted: 17 September 2024 doi:10.20944/preprints202409.1337.v

Disclaimer/Publisher's Note: The statements, opinions, and data contained in all publications are solely those of the individual author(s) and contributor(s) and not of MDPI and/or the editor(s). MDPI and/or the editor(s) disclaim responsibility for any injury to people or property resulting from any ideas, methods, instructions, or products referred to in the content.

Article

Exploring the Application of Advanced Chromatographic Methods to Characterize the Surface Physicochemical Properties and Transition Phenomena of Polystyrene-*b*-Poly(4-vinylpyridine)

Tayssir Hamieh [1,2,*]

[1] Faculty of Science and Engineering, Maastricht University, P.O. Box 616, 6200 MD Maastricht, The Netherlands;

[2] Laboratory of Materials, Catalysis, Environment and Analytical Methods (MCEMA), Faculty of Sciences, Lebanese University, Beirut P.O. Box 6573/14, Lebanon

* Correspondence: t.hamieh@maastrichtuniversity.nl, Tel.: +31 6 5723 9324.

Abstract: The linear diblock copolymer polystyrene-*b*-poly(4-vinylpyridine) (PS-P4VP) is an important copolymer recently used in many applications such as optoelectronics, sensors, catalysis, membranes, energy conversion, energy storage devices, photolithography, and biomedical applications. (1) Background: The surface thermodynamic properties of PS-P4VP copolymer are of great importance in many chemical and industrial processes. (2) Methods: The inverse gas chromatography (IGC) at infinite dilution was used for the experimental determination of the retention volumes of organic solvents adsorbed on copolymer surfaces as a function of temperature. This led to the variations of the free energy of interaction necessary to the evaluation of the London dispersive and polar acid-base surface energies, the polar enthalpy and entropy, the Lewis acid-base constants, and the transition temperatures of PS-P4VP copolymer. (3) Results: The application of the thermal Hamieh model led to accurate determination of the London dispersive surface energy of the copolymer that showed non-linear variations versus the temperature highlighting the presence of two transition temperatures. It was observed that the Lewis's acid-base parameters of the copolymer strongly depend on the temperature and the Lewis base constant of the solid surface was showed to be higher than the its acid constant. (4) Conclusions: Un important effect of the temperature on the surface thermodynamic properties of PS-P4VP was proved and new surface correlations were determined.

Keywords: Adsorption; London dispersion interaction; dispersive and polar free surface energy; enthalpy and entropy of adsorption; Hamieh thermal model; glass transition; Lewis's acid-base surface energies

1. Introduction

Block copolymers are considered as a special class of polymers in the large family of soft matter [1], consisting of at least two fragments of different chemical nature of the polymer, joined together by a junction – type of covalent bond and can be easily synthetized by various polymerization techniques [2-5]. The advantage of the block copolymers resides in the coupling of two polymers and combining their divergent properties differing in a single structure. Block copolymers are widely used as self-assembling polymer materials that provide access to a variety of periodic nanoscale morphologies with feature sizes ranging from 5 to 50 nm [6,7].

Many works were devoted to block copolymers because of their self-assembly into 2- or 3-dimensional periodic nanostructures, such as spherical, cylindrical, lamellar, gyroid structures [8-12], and the crucial interest of the control of their surface structure and uses in many areas of science and technology where surface properties play an important role due to their uniformity, spatial regularity at the nanometric scale [13], and versatile nanoscale fabrication tool for semiconductor devices and other applications [14,15]. The block copolymers have received considerable attention due to their

© 2024 by the author(s). Distributed under a Creative Commons CC BY license.

Preprints.org (www.preprints.org) | NOT PEER-REVIEWED | Posted: 17 September 2024 doi:10.20944/preprints202409.1337.v

ability to microphase separate into various nanostructures when studied in bulk and/or thin films. The important contribution to their self-assembly results in the immiscibility between the different covalently connected segments and their application towards the fabrication of high-resolution patterns for nanolithography applications. Recent advances in directed self- assembly of block copolymers enable low defect density, extremely minimal dimensions, facile processability, etching selectivity, low-cost and ability to design various patterns [16,17]. The periodic ordered microphase separation structures at the molecular chain scale formed by block copolymers, are ideal materials for self-assembly of structured particles and for fabricating polymer particles with adjustable shapes, internal phase structures and surface characteristics [18,19].

The block copolymers, due to their high periodicity, feature and precise size, were used in many applications such as optoelectronics, photonics, sensors, field emission, catalysis, membranes, energy conversion, energy storage devices, photolithography, nanomedicine, and biomedical applications for the diagnosis and treatment of a variety of diseases [20-34]. They also served as templates for the deposition of inorganic materials [25]. The solvent-mediated infiltration of different oxidation state metal cations selectively inserted into self-assembled block copolymer nanopatterns formed from polystyrene-*b*-poly(4-vinylpyridine) (PS-*b*-P4VP) thin films. It was observed that the stability of the as-obtained metal-pyridine complex is highly influenced by the coordination chemistry of the metal ion and the P4VP group and this impacts the formation of metal oxide patterns [26]. Shevate et al. [35] used the PS-*b*-P4VP copolymer to obtain isoporous block copolymer membranes by non-solvent induced phase separation and showed highly ordered surface layer, high flux and superior separation properties and a strong flux dependence of pH; pores closed at low pH and opened at high pH. A unique perforated lamellar (PL) morphology was observed by Singh et al. [36] in a mixture of an asymmetric PS-*b*-P4VP block copolymer and CdSe–CdS quantum dots (QDs). The PL morphology formed by the PS-*b*-P4VP/CdSe–CdS composites consisted of alternating layers of PS and P4VP, where the layer formed by the minority PS block contained cylindrical perforations of the majority P4VP block. The thermal and rheological properties of PS-*b*-P4VP diblock copolymers were studied by Xue et al. [37] and Schultze et al [38] in order to get information about the optimum foaming temperature. PS-b-P4VP was also to identify the constructional details of the polymer thin film morphology [39].

The important and interesting uses and applications of PS-b-P4VP copolymer, particularly in the field of nanotechnology, nanolithography, nanodevices, and materials science, imply the necessity of the determination of the surface physicochemical properties of PS-b-P4VP copolymer. Because of the important lack in this domain, this research work was devoted to an accurate evaluation of the surface thermodynamic properties of this copolymer, such as the London dispersive surface energy, the free dispersive and polar interaction energy, the Lewis's acid-base parameters, and the transition temperatures of PS-b-P4VP diblock copolymer as a function of the temperature. To do that, the inverse gas chromatography (IGC) technique at infinite dilution [40-52] was used by applying our new methodology based on the thermal hamieh model and the London dispersion interaction that were proved to give more accurate surface parameters of solid surfaces [53-63].

2. Materials and Methods

2.1. Solvents and Materials

All chemicals were purchased from Sigma-Aldrich (Beirut, Lebanon): the non-polar organic solvents such as *n*-Hexane, *n*-heptane, *n*-octane, benzene, and the polar molecules, such as dichloromethane, chloroform, and carbon tetrachloride (Lewis's acid solvents); ethyl acetate, acetone, and tetrahydrofuran (Lewis's base solvents); and ethanol and acetonitrile (amphoteric solvents). The polystyrene-*b*-poly(4-vinylpyridine) was previously synthetized [64] through atom transfer radical polymerization (ATRP) with a number average molecular weight equal to Mn= 41,000 g mol^{-1}were from molecular weights of PS and P4VP blocks respectively equal to Mn= 41,000 and 5200 g mol^{-1}.

2.2. Inverse Gas Chromatography

Preprints.org (www.preprints.org) | NOT PEER-REVIEWED | Posted: 17 September 2024 doi:10.20944/preprints202409.1337.v

The net retention time of organic solvents adsorbed on polystyrene-*b*-poly(4-vinylpyridine) copolymer was determined at different temperatures using inverse gas chromatography at infinite dilution with the help of a Focus GC gas chromatograph equipped with a flame ionization detector of high sensitivity (Sigma-Aldrich, France). A mass of 1 g of PS-b-P4VP diblock copolymer was packed into a stainless-steel column of length 30 cm and 2 mm internal diameter. Helium was used as carrier gas with a flow rate equal to 25 mL/min. The retention times of the different injected organic solvents, measured at infinite dilution, led to the interactions between the organic molecules and the polymer, supposing that there is no interaction between the probe molecules themselves. The column temperatures varied from 30 to 200 °C. Average retention times and volumes were determined by repeating three times each solvent injection with a standard deviation less than 1% in all chromatographic measurements.

2.3. Thermodynamic Methods

2.3.1. Fundamental Equation of IGC

The fundamental equation of the inverse gas chromatography at infinite dilution can be written as follows:

$$\Delta G_a^0(T) = -RTlnVn(T) + C(T) \quad (1)$$

where $\Delta G_a^0(T)$ is the free energy of adsorption of organic solvents on the solid materials, Vn the net retention volume, T the absolute temperature, R the perfect constant gas, and $C(T)$ a constant depending on the temperature and the interaction solvents-sorbent.

The IGC experiments allow obtaining the values of $RTlnVn(T)$ of the adsorbed probes at different temperatures and consequently the free energy of interaction.

When non-polar solvents such as n-alkanes are adsorbed on the copolymer, $\Delta G_a^0(T)$ is only equal to the London dispersive energy $\Delta G_a^d(T)$ at any temperature, and one writes:

$$\Delta G_a^0(T) = \Delta G_a^d(T) \quad (2)$$

However, by using polar solvents, Equation 3 can be therefore written:

$$\Delta G_a^0(T) = \Delta G_a^d(T) + \Delta G_a^p(T) \quad (3)$$

with $\Delta G_a^p(T)$ the free polar energy of the polar probes.

2.3.2. London Dispersive Surface Energy of Solid Surfaces

In a first attempt, Dorris-Gray [65] determined the London dispersive component γ_s^d of the surface energy of the solid material using the Fowkes's relation [66]. The obtained relation giving $\gamma_s^d(T)$ is the following:

$$\gamma_s^d = \frac{\left[RTln\left[\frac{Vn\left(C_{n+1}H_{2(n+2)}\right)}{Vn\left(C_nH_{2(n+1)}\right)}\right]\right]^2}{4\mathcal{N}^2\, a_{-CH2-}^2\, \gamma_{-CH2-}} \quad (4)$$

Where $C_nH_{2(n+1)}$ and $C_nH_{2(n+1)}$ are two consecutive n-alkanes, a_{-CH2-}, the surface area of methylene group with $a_{-CH2-} = 6$Å, independent from the temperature, and the surface energy γ_{-CH2-} of methylene group was given by:

$$\gamma_{-CH2-}(\text{in mJ/m}^2) = 52.603 - 0.058\,T\ (T\ in\ K) \quad (5)$$

A second method using the same Fowkes concept was proposed in literature [44] and also led to γ_s^d of solid surfaces (Equation 6):

$$RTln(Vn) = 2\mathcal{N}a\left(\gamma_l^d\gamma_s^d\right)^{1/2} + \alpha(T) \quad (6)$$

Where a is the surface area of an adsorbed molecule (previously supposed constant), $\mathcal{N}$ the Avogadro number and $\alpha(T)$ a constant only depending on the temperature and the solid substrate.

Preprints.org (www.preprints.org) | NOT PEER-REVIEWED | Posted: 17 September 2024 doi:10.20944/preprints202409.1337.v

A first criticism was addressed to the above methods by hamieh et al. [50] that proved that the London dispersive surface energy of the solvents γ_l^d depended on the temperature and proposed several molecular models allowing the determination of the surface areas of molecules and then the surface area of methylene group for each model. The following models were used: geometric model based on the real form of molecules, cylindrical model based on cylindrical form of molecules, spherical model based on spherical form of molecules. Kiselev results, the two-dimensional Van der Waals (VDW) equation, and the two-dimensional Redlich-Kwong (R-K) equation [50].

The second serious criticism was formulated by the Hamieh thermal model proving in recent works that the surface area of organic solvents strongly depends on the temperature [53-56,59,60], and this thermal influence effectively modifies the different values of the surface parameters of solid substrates such as γ_s^d, ΔG_a^p and the Lewis acid-base surface energies and variables. New equation giving the variation of the surface area $a(T)$ of polar and non-polar molecules were proposed against the temperature, as well as the expression of surface area of methylene group $a_{-CH2-}(T)$ [53-56,59,60]. The linear relations of γ_l^d of the various were also given.

The surface energetic parameters of PS-b-P4VP diblock copolymer were determined using our new thermal model taking into account the variations of $a(T)$ and $\gamma_l^d(T)$ of the probes versus the temperature.

2.3.3. London Dispersive and Polar Free Energies of Adsorption

Several chromatographic methods were used in the literature to determine the London dispersive and polar free energies of solids [41,44-50]. The various methods were based on the use of several reference thermodynamic parameters such as the boiling point $T_{B.P.}$ of the solvents [41], the vapor pressure P_0 of the probes at a fixed temperature [45,46]

- the dispersive component γ_l^d of the surface energy of the solvent [44], the deformation polarizability α_0 [47], the topological index χ_T of the solvents [48,49].
- It was proved that these various methods cannot be considered as accurate quantitative methods that allow an accurate separation between the dispersive and polar free energies of adsorption and the only method theoretically well-founded was that based on the deformation polarizability. However, this method was not well-applied, because the authors did some approximations that led to wrong values of the polar contribution of the free energy of interaction between the solvents and the solid materials.

To better determine the two dispersive and polar of the free energies of solvents adsorbed on the PS-b-P4VP diblock copolymer, our new methodology [53-56,59,60] based on the London dispersion interaction energy was applied (Equation 7):

$$\Delta G_a^d(T) = -\frac{\alpha_{0S}}{H^6}\left[\frac{3\mathcal{N}}{2(4\pi\varepsilon_0)^2}\left(\frac{\varepsilon_S\,\varepsilon_X}{(\varepsilon_S+\varepsilon_X)}\alpha_{0X}\right)\right] \quad (7)$$

Where ε_0 is the dielectric constant of vacuum, α_{0S} and α_{0X} the respective deformation polarizabilities of the solid material denoted by S and the organic solvent denoted by X, separated by a distance H, and ε_S and ε_X their corresponding ionization energies.
By combining Equations 1, 3, and 7, one obtained the following relation:

$$RTlnVn = \frac{\alpha_{0S}}{H^6}\left[\frac{3\mathcal{N}}{2(4\pi\varepsilon_0)^2}\left(\frac{\varepsilon_S\,\varepsilon_X}{(\varepsilon_S+\varepsilon_X)}\alpha_{0X}\right)\right] - \Delta G_a^p(T) + C(T) \quad (8)$$

A new chromatographic interaction parameter $\mathcal{P}_{SX}$ was chosen:

$$\mathcal{P}_{SX} = \frac{\varepsilon_S\,\varepsilon_X}{(\varepsilon_S+\varepsilon_X)}\alpha_{0X} \quad (9)$$

In the case of non-polar molecules such as n-alkanes, the variations of $RTlnVn$ of the solvents were obtained from Equation 10:

Preprints.org (www.preprints.org) | NOT PEER-REVIEWED | Posted: 17 September 2024 doi:10.20944/preprints202409.1337.v

$$\begin{cases} RTlnVn(non-polar) = A\left[\frac{3\mathcal{N}}{2(4\pi\varepsilon_0)^2}\mathcal{P}_{SX}(non-polar)\right] + C(T) \\ A = \frac{\alpha_{0S}}{H^6} \end{cases} \quad (10)$$

where A is the slope of the non-polar straight line which is function of the separation distance between solid surface and organic molecules.

The free polar energy $\Delta G_a^p(polar)$ of polar molecules adsorbed on the diblock copolymer were then obtained as a function of the temperature using Equation 11:

$$\Delta G_a^p(T, polar) = RTlnVn\,(T, polar) - A\left[\frac{3\mathcal{N}}{2(4\pi\varepsilon_0)^2}\mathcal{P}_{SX}(polar)\right] - C(T) \quad (11)$$

2.3.4. Lewis's Acid-Base Parameters of PS-b-P4VP Diblock Copolymer

The experimental determination of $\Delta G_a^p(T, polar)$ was used to obtain the values of polar enthalpy $(-\Delta H_a^p)$ and entropy $(-\Delta S_a^p)$ of polar probes adsorbed on the PS-*b*-P4VP diblock copolymer. The relation 12 was used when the linearity of $\Delta G_a^p(T)$ is satisfied.

$$\Delta G_a^p(T) = \Delta H_a^p - T\Delta S_a^p \quad (12)$$

However, in many cases of the interaction between polymers and organic solvents, the linearity was not insured. The values of $(-\Delta H_a^p(T))$ and $(-\Delta S_a^p(T))$ were then determined from the following thermodynamic equations:

$$\begin{cases} \Delta H_a^{sp}(T) = \frac{\partial\left(\frac{\Delta G_a^{sp}(T)}{T}\right)}{\partial\left(\frac{1}{T}\right)} \\ \Delta S_a^{sp}(T) = -\left(\frac{\partial\left(\Delta G_a^{sp}(T)\right)}{\partial T}\right) \end{cases} \quad (13)$$

The classic relations 14 were used to determine the variations of the Lewis's acid-base parameters of PS-*b*-P4VP copolymer as a function of the temperature. Their enthalpic (K_A, K_D) and entropic (ω_A, ω_D) acid-base parameters were therefore determined:

$$\begin{cases} (-\Delta H^p) = K_A \times DN' + K_D \times AN' \\ (-\Delta S_a^p) = \omega_A \times DN' + \omega_D \times AN' \end{cases} \quad (14)$$

where $DN'$and $AN'$are, respectively, the corrected electron donor and acceptor numbers of the polar molecule [67,68].

2.3.4. Lewis's Acid-Base Surface Energies of PS-b-P4VP Copolymer

The application of the Hamieh thermal model led to the London dispersive surface energy $\gamma_s^d(T)$ of PS-*b*-P4VP copolymer against the temperature. However, the total surface energy $\gamma_s^{tot.}$ of a solid surface is given by:

$$\gamma_s^{tot.} = \gamma_s^d + \gamma_s^p \quad (14)$$

where $\gamma_s^p = \gamma_s^{AB}$ represents the polar (or acid-base) contribution of the surface energy.

The determination of γ_s^p was obtained using Van Oss et al.'s method [69], it was possible to determine γ_s^p of PS-*b*-P4VP copolymer. The polar surface energy of the copolymer is given by:

$$\gamma_s^p = 2\sqrt{\gamma_s^+\gamma_s^-} \quad (15)$$

where γ_s^+ and γ_s^- are respectively the Lewis acid and base surface energies of the solid material.

Van Oss et al. [69] used two solvents such as ethyl acetate (base *B*) and dichloromethane (acid *A*), characterized by the following parameters:

$$\begin{cases} \gamma_A^+ = 5.2\ \text{mJ/m}^2, \gamma_A^- = 0 \\ \gamma_B^+ = 0\ , \gamma_B^- = 19.2\ \text{mJ/m}^2 \end{cases} \quad (16)$$

Preprints.org (www.preprints.org) | NOT PEER-REVIEWED | Posted: 17 September 2024 doi:10.20944/preprints202409.1337.v

Knowing that the polar free energy $\Delta G_a^p(T)$ of the polar solvents are given by:

$$\Delta G_a^p(T) = 2\mathcal{N}a(T)\left(\sqrt{\gamma_l^-\gamma_s^+} + \sqrt{\gamma_l^+\gamma_s^-}\right) \quad (17)$$

therefore, the Lewis acid and base surface energies of the copolymer can be obtained from Equations 18:

$$\begin{cases} \gamma_s^+(\mathrm{T}) = \dfrac{\left[\Delta G_a^p(T)\,(B)\right]^2}{4\mathcal{N}^2[a_B(T)]^2\gamma_B^-} \\ \gamma_s^-(\mathrm{T}) = \dfrac{\left[\Delta G_a^p(T)\,(A)\right]^2}{4\mathcal{N}^2[a_A(T)]^2\gamma_A^+} \end{cases} \quad (18)$$

Equations 18, 15, and 14 led to the values of the polar and total surface energies of the copolymer.

3. Experimental results

3.1. Variations of $RT\ln Vn(T)$ of solvents adsorbed on PS-b-P4VP diblock copolymer

The values of $RT\ln Vn(T)$ of n-alkanes and polar solvents adsorbed on the PS-*b*-P4VP diblock copolymer were given in Tables S1 and S2 ((Supplementary Materials) and the variations were plotted in Figure 1.

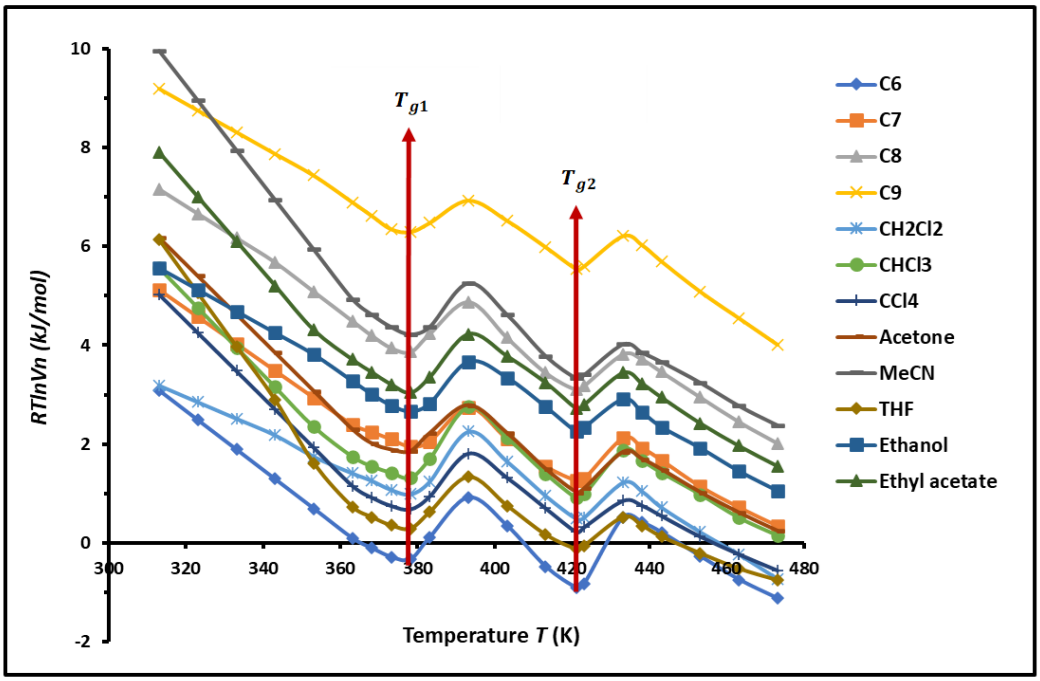

Figure 1. Variations of $RT\ln Vn$ (kJ/mol) of n-alkanes and polar solvents adsorbed on PS-*b*-P4VP diblock copolymer as a function of temperature.

The non-linear evolution of $RT\ln Vn$ of the different organic molecules adsorbed on PS-P4VP diblock copolymer against the temperature, drawn in Figure 1 showed the presence of two minima for all used solvents at the respective temperatures T_{g1} = 378.15K and T_{g2} = 421.15K. These two particular temperatures perfectly correspond to the respective transition temperatures of PS and P4VP. This interesting result proved that the block copolymers behave as separated phases.

The transition temperatures of PS-*b*-P4VP diblock copolymer were studied by several authors using differential scanning calorimetry (DSC) [38,70-75]. Zhang et al. [70] showed that the pure PSb-P4VP copolymer exhibits two glass transition temperatures: one T_g of PS is 100.88°C and the other is the T_g of P4VP at 130.98°C largely depending on the ratio of the molecular masses of PS on P4VP blocks. Whereas, other values of T_g of P4VP (T_g = 138 ◦C) was showed by Zhao et al. [71]. The ratio of number molecular weights of PS on P4VP varied between 30% and 50%.

Preprints.org (www.preprints.org) | NOT PEER-REVIEWED | Posted: 17 September 2024 doi:10.20944/preprints202409.1337.v

However, the glass transition temperature T_g of the PS and P4VP of the diblock copolymer was analyzed by Schulze et al. [38] using DSC technique. They highlighted two glass transitions of approximately 105 °C for polystyrene and 150 °C for poly(4-vinylpyridine). The same values of T_g were obtained by Rahikkala et al. [74]. The DSC measurements on the PSb-P4VP block copolymers carried out by Huang et al. [75] also exhibited two glass transitions, indicating that the resulting block copolymers are phase separated and reporting two T_{gs} for PS and P4VP blocks in the PSb-P4VP copolymer respectively equal to 100 °C, and 150 °C for a ratio of number molecular weights of PS on P4VP equal to 20%. These two transition temperatures are obviously, quite similar to those of respective homopolymers indicating that the resulting block copolymers are phase separated in condensed state [75].

The results of T_g obtained by this work ($T_{g1} = 105$ °C and $T_{g2} = 148$ °C) are very close to those obtained by Schulze et al. [38], Rahikkala et al. [74], and Huang et al. [75] with a small deviation not exceeding 5% due to the difference observed in the molecular weight and composition of the blocks.

3.2. London Dispersive Surface Energy of PS-b-P4VP diblock copolymer

Using the results given in Tables S1 and S2, and the Hamieh thermal model [53-56], it was possible to determine the Londo dispersive surface energy $\gamma_s^d(T)$ of PS-*b*-P4VP diblock copolymer as a function of the temperature. The results were given in Figure 2.

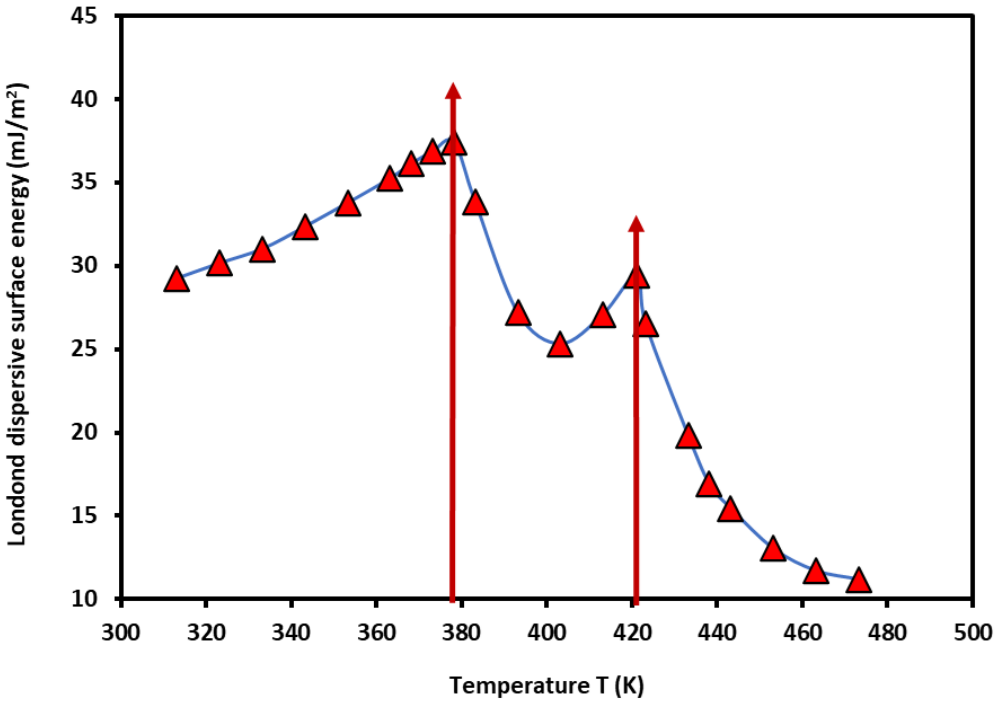

Figure 2. Variations of the London dispersive surface energy γ_s^d (mJ/m^2) of PS-b-P4VP diblock copolymer as a function of the temperature *T* (K) using the Hamieh thermal model.

The non-linear variations of the London dispersive surface energy showed two maxima corresponding to the two glass transition temperatures of PS and P4VP blocks in PS-*b*-P4VP diblock copolymer then confirming those previously obtained in Figure 1:

- $T_{g1} = 105$ °C relative to PS glass transition

- $T_{g2} = 148$ °C relative to P4VP glass transition

In several previous studies [50,61-63], the transition temperatures of some polymers in bulk and adsorbed phases were highlighted by IGC technique. An important effect of the temperature, the polymer tacticity, and the recovery fraction was showed on the values of the second order transition

Preprints.org (www.preprints.org) | NOT PEER-REVIEWED | Posted: 17 September 2024 doi:10.20944/preprints202409.1337.v

temperatures. The variations of $\gamma_s^d(T)$ of PS-*b*-P4VP diblock copolymer are constituted by three parabolic functions given in Table 1 and represented by the following general equation with an excellent linear regression coefficient ($R^2 > 0.99$):

$$\gamma_s^d(T) = aT^2 + bT + c \quad (19)$$

Table 1. Equations of $\gamma_s^d(T)$ of PS-*b*-P4VP diblock copolymer with the linear regression coefficients in the corresponding temperature interval.

Equation of $\gamma_s^d(T)$	R^2	Temperature interval
$\gamma_s^d(T) = 7.10^{-4}T^2 - 0.324T + 66.3$	0.9983	313.15K - 378.15K
$\gamma_s^d(T) = 1.7.10^{-2}T^2 - 13.733T + 2806$	0.9910	378.15K - 421.15K
$\gamma_s^d(T) = 9.1.10^{-3}T^2 - 8.465T + 1979$	0.9914	421.15K - 473.15K

The results in Table 1 confirmed the general tendency of the variations of the London dispersive surface energy of polymers obtained in the case of transition phenomena of Poly(methyl methacrylate) (PMMA) [50,61-63]. For the PS-*b*-P4VP diblock copolymer, it was proved that the two glass transition temperatures correspond to those of PS and P4VP separately taken with slight variation. In the case of first order linear interpolation in the considered temperature interval [313.15K - 473.15K], a bad linear correlation, $R^2 = 0.6456$, was obtained, certainly due to non-linearity of the function $\gamma_s^d(T)$. The corresponding $\gamma_s^d(T)$ of PS-b-P4VP diblock copolymer is given by the following relation:

$$\gamma_s^d(T) = -0.147T + 84.50 \quad (20)$$

The useful information obtained by this large approximation was the determination of the following surface energetic parameters of PS-b-P4VP diblock copolymer:

- the surface entropy: $S_s = -\frac{d\gamma_s^d}{dT} = 0.147 \text{ mJ} \times \text{m}^{-2} \times \text{K}^{-1}$,
- the London dispersive energy at 0K: $\gamma_s^d(0K) = 84.50 \text{ mJ} \times \text{m}^{-2}$,
- the intrinsic temperature $T_{int.} = \gamma_s^d(0K)/S_s = 574.8$ K.

The above values can be compared to those obtained in other works on PMMA [61-63], with smaller surface parameter values of PS-*b*-P4VP diblock copolymer, but higher intrinsic temperature.

3.3. Polar free surface energy of PS-b-P4VP diblock copolymer

By applying our new methodology using the London dispersion interaction equation, the results given in Tables S1 and S2, and the values of the deformation polarizability α_{0X} and the ionization energies [76] of the various n-alkanes and polar molecules adsorbed on the PS-b-P4VP diblock copolymer, Equation 11 led to the variations of the free polar surface energy ($-\Delta G_a^p(T)$) of polar solvents adsorbed on the copolymer as a function of the temperature. The values of ($-\Delta G_a^p(T)$) were given in Table S3 and the curves were plotted in Figure 3. A large difference in the values of the free polar energy was observed with the various polar solvents adsorbed on PS-b-P4VP diblock copolymer. The polar probes can be globally classified in increasing order of their polar interaction energy as follows:

$CHCl_3$ < CH_2Cl_2 < THF < MeCN < CCl_4 < ethyl acetate < ethanol < acetone showing the highest polar free energy with Lewis's base solvents.

Non-linear variations of ($-\Delta G_a^p(T)$) of the different polar molecules were also observed due to the reorganization of the surface groups of the copolymer blocks and highlighted the two glass transition temperatures of PS-*b*-P4VP diblock copolymer with small fluctuations of the polar interaction energy as a function of the temperature (Figure 3).

Preprints.org (www.preprints.org) | NOT PEER-REVIEWED | Posted: 17 September 2024 doi:10.20944/preprints202409.1337.v

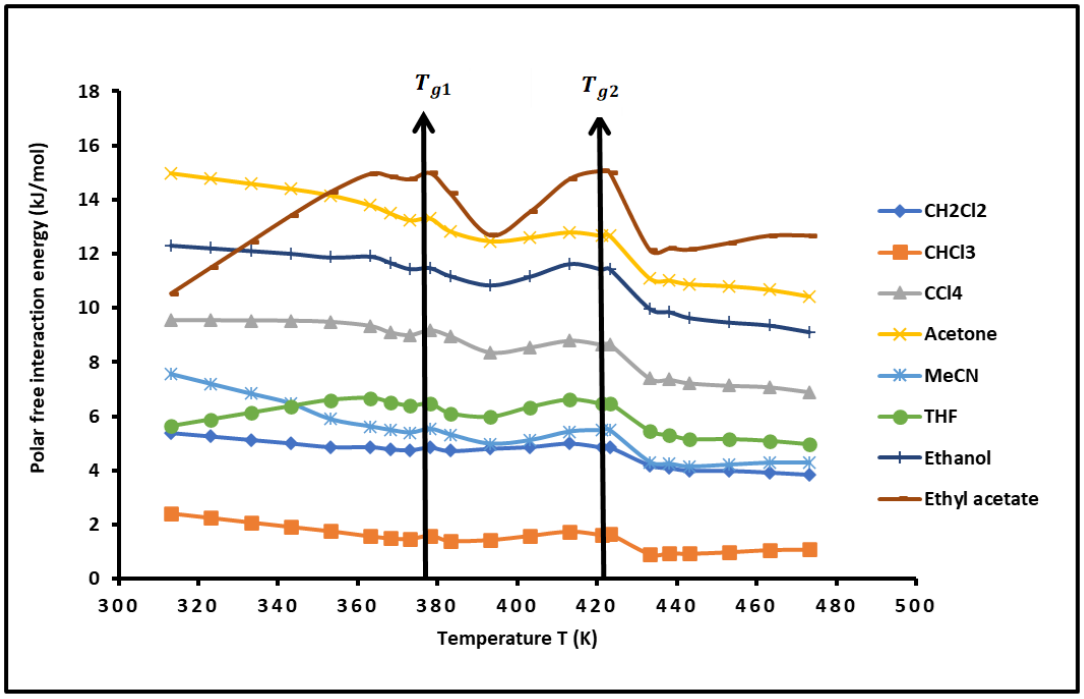

Figure 3. Evolution of the polar free interaction energy $(-\Delta G_a^p(T))$ (kJ/mol) of different polar solvents adsorbed on PS-b-P4VP diblock copolymer.

3.4. Polar enthalpy and entropy of adsorption

The results presented in Table S3 giving the non-linear variations of $(-\Delta G_a^p(T))$of adsorbed solvents on PS-b-P4VP diblock copolymer and the Equations 13 allowed determining the values of the polar enthalpy $(-\Delta H_a^p(T))$ (Table S4) and entropy $(-\Delta S_a^p(T))$ (Table S5) of adsorption of polar probes on the copolymer as a function of the temperature. The results were plotted in Figure 4. The variations of $(-\Delta H_a^p(T))$ showed the adsorption and desorption phenomena of the polar molecules on the copolymer surface with a stronger tendency to the adsorption and sever and non-linear fluctuations as a function of the temperature due to the presence of the glass transition affecting the group reorganization and rearrangement when the temperature is very close to the transition phenomena. Whereas, brutal variations of the polar entropy change $(-\Delta S_a^p(T))$ of the adsorbed with a certain disorder near the transition temperatures and more ordered and organized surface of the copolymer far from these transition temperatures. Some solvents such THF and ethyl acetate showed higher disorder of interaction with the PS-*b*-P4VP diblock copolymer. The maximum of disorder was observed at the two transition temperatures for all polar molecules.

Preprints.org (www.preprints.org) | NOT PEER-REVIEWED | Posted: 17 September 2024 doi:10.20944/preprints202409.1337.v

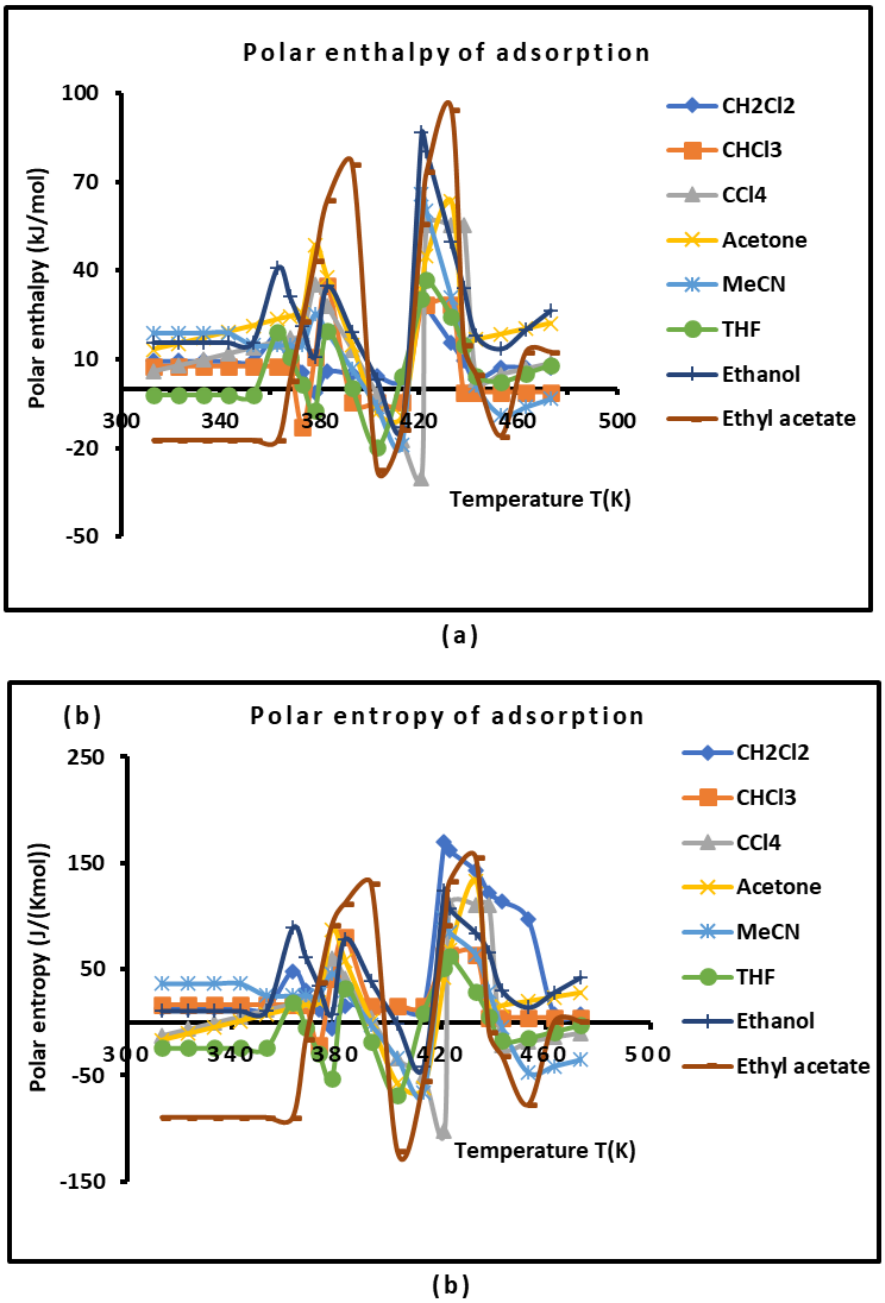

Figure 4. Variations of the polar interaction enthalpy $(-\Delta H_a^p(T)\,(kJ/mol)$ (a) and entropy $(-\Delta S_a^p(T))\,(JK^{-1}mol^{-1})$ (b) of polar solvents adsorbed on PS-*b*-P4VP diblock copolymer.

The non-linearity variations of $(-\Delta H_a^p(T))$ and $(-\Delta S_a^p(T))$ of the different adsorbed solvents observed as a function of temperature led to important variations of the Lewis's acid-base properties of the PS-b-P4VP diblock copolymer against the temperature. However, the calculations of the average values $(-\Delta H_a^p)$ and $(-\Delta S_a^p)$ of the various polar molecules allowed obtaining the results in Table 2.

Table 2. Equations of the average polar free energy $(-\Delta G_a^p(T))$ and average values of the polar entropy and enthalpy of adsorption with the corresponding linear regression coefficients.

Solvent	Equation of $(-\Delta G_a^p(T))$ (kJ/mol))	$(-\Delta S_a^p)$ (J/k.mol)	$(-\Delta H_a^p)$ (kJ/mol))	R^2
CHCl3	$(-\Delta G_a^p(T))$ = -0.0086T + 8.083	8.6	8.083	0.7739
CH2Cl2	$(-\Delta G_a^p(T))$ = -0.0079T + 14.074	7.9	14.074	0.7529

Preprints.org (www.preprints.org) | NOT PEER-REVIEWED | Posted: 17 September 2024 doi:10.20944/preprints202409.1337.v

THF	$(-\Delta G_a^p(T))$ = -0.0186T + 1.733	18.6	1.733	0.8626
MeCN	$(-\Delta G_a^p(T))$ = -0.018T + 24.538	18.0	24.538	0.9422
CCl4	$(-\Delta G_a^p(T))$ = -0.0195T + 13.095	19.5	13.095	0.8499
Ethyl acetate	$(-\Delta G_a^p(T))$ = -0.0071T + 8.773	7.1	8.773	0.423
Ethanol	$(-\Delta G_a^p(T))$ = -0.020T + 18.952	20.0	18.952	0.8176
Acetone	$(-\Delta G_a^p(T))$ = 0.0084T + 13.14	8.4	13.140	0.3215

The results in Table 2 showed that the linear regression coefficients are generally very bad because of the extreme non-linearity previously observed in Figures 3 and 4.

3.5. Temperature Effect on the Lewis's Acid-Base Parameters of the Copolymer

Using equations 14 and the values of $(-\Delta H_a^p(T))$ and $(-\Delta S_a^p(T))$ given in Tables S4 and S5, one determined the Lewis enthalpic acid base parameters K_A and K_D and the entropic acid base parameters ω_A and ω_D of the PS-b-P4VP diblock copolymer as a function of the temperature. The evolution of the various enthalpic and entropic acid-base parameters of the PS-*b*-P4VP diblock copolymer as a function of the temperature was plotted in Figure 5. It was showed that the diblock copolymer exhibited very stronger Lewis's base character reaching at certain temperatures 20 times higher than its Lewis acidity. The basicity of the copolymer was proved to be maximum at the glass transition. An important non-linearity of the different Lewis's acid-base parameters the PS-*b*-P4VP diblock copolymer was observed (Figure 5) when the temperature varied. This is essentially due to the presence of the glass transitions that participate to the acid and base group reorganization controlling at the same time the variations of the acid-base properties of the copolymer.

The calculations of the average values of $(-\Delta H_a^p(T))$ and $(-\Delta S_a^p(T))$ of the adsorbed polar molecules by applying Equations 14 gave in Table 3 the following average values of the acid base constants independently from the temperature.

Table 3. Average values of the various enthalpic and entropic Lewis's acid-base parameters of the PS-b-P4VP diblock copolymer with the corresponding linear regression coefficients.

Lewis's acid-base parameter	Average values	R^2
K_A	0.092	0.8556
K_D	0.693	0.8556
K_D/K_A	7.533	0.8556
$(K_D + K_A)$	0.785	0.8556
$10^3 \times \omega_A$	0.06	0.6732
$10^3 \times \omega_D$	1.0	0.6732
ω_D/ω_A	18.18	0.6732
$10^3 \times (\omega_D + \omega_A)$	1.06	0.6732

Table 3 showed that the PS-*b*-P4VP diblock copolymer exhibits then a stronger Lewis base character which is globally 7.5 times more basic than acidic. The evolution of the Lewis acid-base of the copolymer also highlighted the presence of the two glass transition temperatures.

Preprints.org (www.preprints.org) | NOT PEER-REVIEWED | Posted: 17 September 2024 doi:10.20944/preprints202409.1337.v

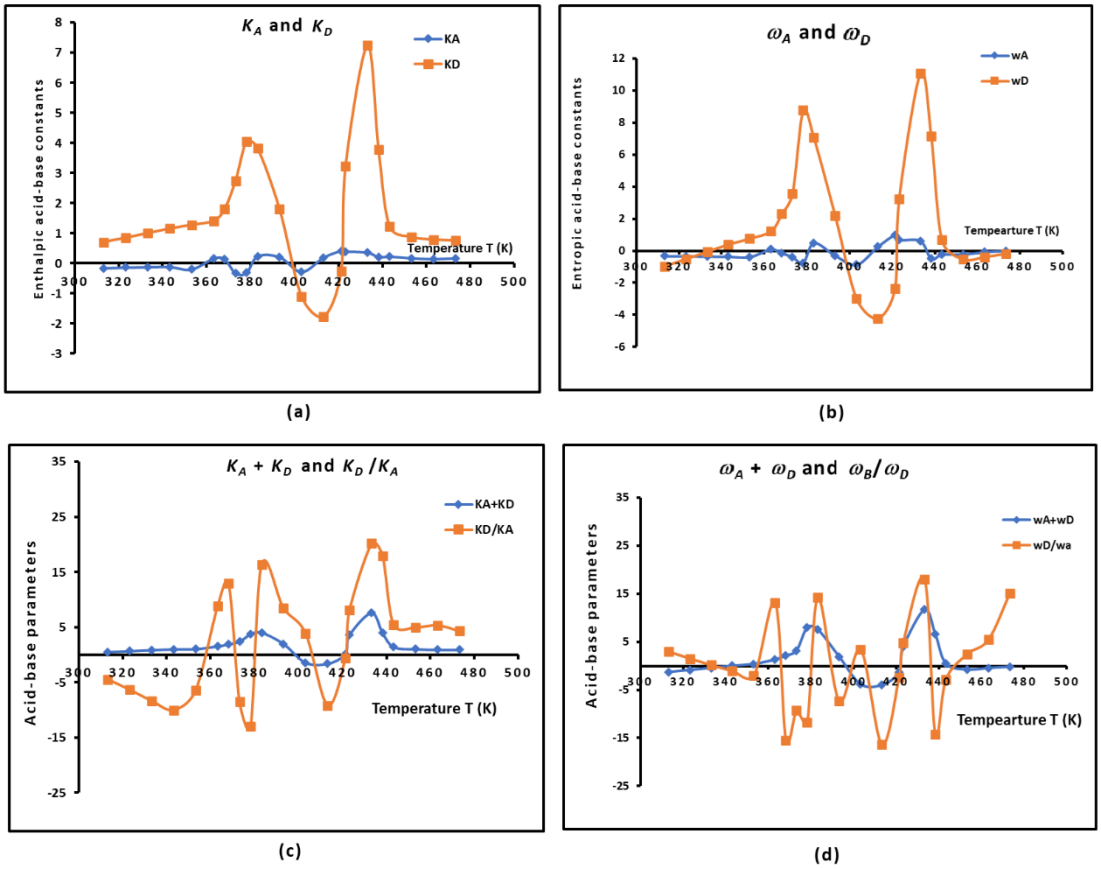

Figure 5. Variations of the various enthalpic and entropic acid-base parameters of the PS-b-P4VP diblock copolymer as a function of the temperature: (a): K_A and K_D, (b): ω_A and ω_D, (c): K_D/K_A and $(K_D + K_A)$; (d): ω_D / ω_A and $(\omega_D + \omega_A)$. The values of ω_A and ω_D given in the figures were multiplied by 10^3.

3.6. Separation Distance, Lewis Acid-Base Surface Energies of PS-b-P4VP Copolymer, and and Polar Surface Energy of Solvents

The values of the average separation distance H between the solvents adsorbed on the copolymer surface were determining using Equations 10. The variations of the separation distance $H(T)$ were plotted in Figure 6 as a function of the temperature. Even if these variations are limited between 5.5 and 6.0 Å, however, it was shown in Figure 6 that the non-linear evolution of $H(T)$ decreased before reaching each glass transition of the PS-*b*-P4VP diblock copolymer and then increased for larger temperatures.

Preprints.org (www.preprints.org) | NOT PEER-REVIEWED | Posted: 17 September 2024 doi:10.20944/preprints202409.1337.v

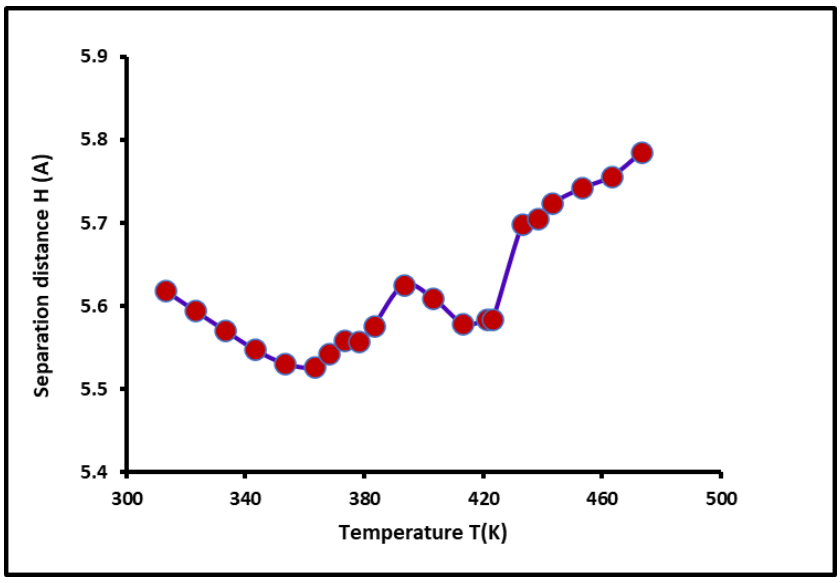

Figure 6. Variations of the separation distance H (T) (Å) of the PS-b-P4VP diblock copolymer a function of the temperature T (K).

Furthermore, the Lewis acid γ_s^+ and base γ_s^- surface energies of the PS-*b*-P4VP diblock copolymer were determined using Equations 20, whereas, the polar acid-base surface energy $\gamma_s^{AB} = \gamma_s^p$ of the copolymer was obtained from Equation 15. While the value of the Lifshitz – Van der Waals (LW) surface energy $\gamma_s^{LW} = \gamma_s^{tot.}$ (or total surface energy of the copolymer) was deduced using equation 14. This led to determine the variations of the various polar acid and base surface energies γ_s^+, γ_s^-, γ_s^p, and $\gamma_s^{tot.}$ of the copolymer (Table 4).

Table 4. Values of the polar acid and base surface energies γ_s^+, γ_s^-, γ_s^p , γ_s^d, and $\gamma_s^{tot.}$ (mJ/m²) of the PS-b-P4VP diblock copolymer as a function of the temperature.

T(K)	γ_s^-	γ_s^+	γ_s^p	γ_s^d	$\gamma_s^{tot.}$
313.15	43.33	15.82	52.36	28.24	80.61
323.15	51.05	14.93	55.21	29.63	84.85
333.15	59.29	14.07	57.77	31.00	88.77
343.15	68.08	13.25	60.07	32.33	92.40
353.15	76.49	12.40	61.59	33.29	94.88
363.15	82.96	12.28	63.84	34.79	98.63
368.15	81.51	11.81	62.05	30.08	92.13
373.15	79.96	11.59	60.87	27.26	88.13
378.15	82.02	12.02	62.79	32.75	95.54
383.15	73.70	11.33	57.81	29.72	87.52
393.15	58.03	11.62	51.94	25.17	77.11
403.15	65.57	11.81	55.66	25.31	80.97
413.15	77.12	12.34	61.69	27.09	88.78
421.15	79.58	11.54	60.60	29.45	90.05
423.15	78.67	11.55	60.30	26.54	86.84
433.15	51.16	8.51	41.73	19.85	61.58
438.15	51.42	8.06	40.72	16.93	57.65
443.15	50.79	7.66	39.45	15.46	54.92
453.15	52.39	7.57	39.82	13.05	52.87
463.15	54.15	7.25	39.63	11.72	51.35
473.15	53.70	6.89	38.48	10.68	49.16

Preprints.org (www.preprints.org) | NOT PEER-REVIEWED | Posted: 17 September 2024 doi:10.20944/preprints202409.1337.v

The comparison between the different surface energy components of the copolymer showed the highest values of polar acid surface energy due to the highest basic character of the surface groups of the copolymer blocks. The results in Table 4 showed that the London dispersive surface energy is equivalent to the half of the polar surface energy of the PS-*b*-P4VP diblock copolymer, whereas, the lowest surface energy was obtained for the basic surface energy component, because of the weaker acid force of the surface groups of the copolymer.

The variations of the various surface energy components plotted in Figure 7.

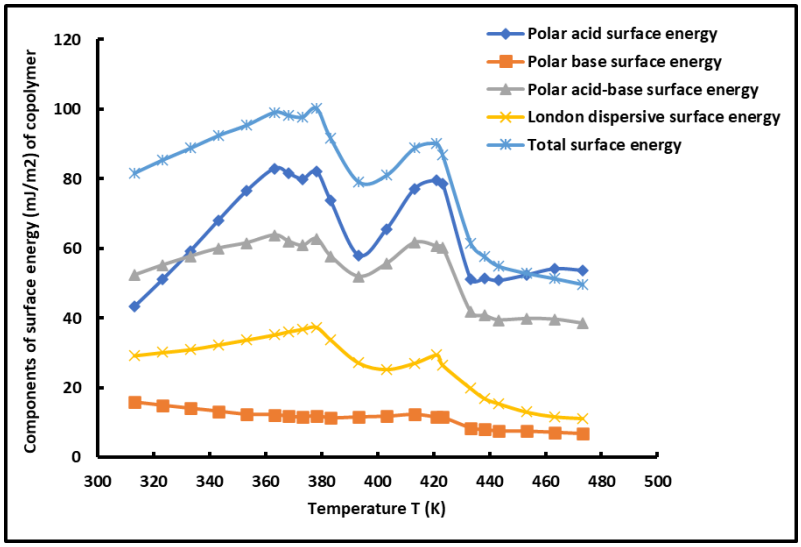

Figure 7. Evolution of the different components of surface energies γ_s^+, γ_s^-, γ_s^p , γ_s^d, and $\gamma_s^{tot.}$ (mJ/m²) of the PS-b-P4VP diblock copolymer as a function of the temperature.

The curves of the different components of the surface energy of the copolymer shown in Figure 7 also confirmed the presence of the two glass transition temperatures of the PS-*b*-P4VP diblock copolymer. The same conclusions were observed in several previous studies [61-63,77].

On the other hand, the experimental results previously obtained allowed determining the polar free energy $(-\Delta G_a^p(X))$ of a polar molecule denoted by X having a surface area a_X and a polar component of the surface energy γ_l^{p}, given by Equation 21:

$$(-\Delta G_a^p(X)) = 2\mathcal{N} a_X \sqrt{\gamma_s^{\mathrm{p}} \gamma_l^{\mathrm{p}}} \quad (21)$$

Knowing the polar surface energy γ_s^{p} of the PS-*b*-P4VP diblock copolymer, the polar surface energy of the organic molecules was determined by Equation 22:

$$\gamma_l^{\mathrm{p}} = \frac{\left(-\Delta G_a^p(X)\right)^2}{4\mathcal{N}^2 a_X{}^2 \gamma_s^{\mathrm{p}}} \quad (22)$$

By varying the temperature, the $\boldsymbol{\gamma_l^{\mathrm{p}}}$ of the various polar solvents adsorbed on the copolymer was determined versus the temperature. The results were plotted in Figure 8. The highest polar contribution of the surface energy of polar molecules was obtained by acetone, respectively followed by ethyl acetate, ethanol, and carbon tetrachloride. A decrease in the values of the $\boldsymbol{\gamma_l^{\mathrm{p}}}$ of the various adsorbed polar solvents was observed when the temperature increased with some variations near the glass temperatures of the copolymer. The curves of Figure 8 highlighted the highest polar surface energy of acetone, certainly due to the highest polarity of this polar solvent.

Preprints.org (www.preprints.org) | NOT PEER-REVIEWED | Posted: 17 September 2024 doi:10.20944/preprints202409.1337.v

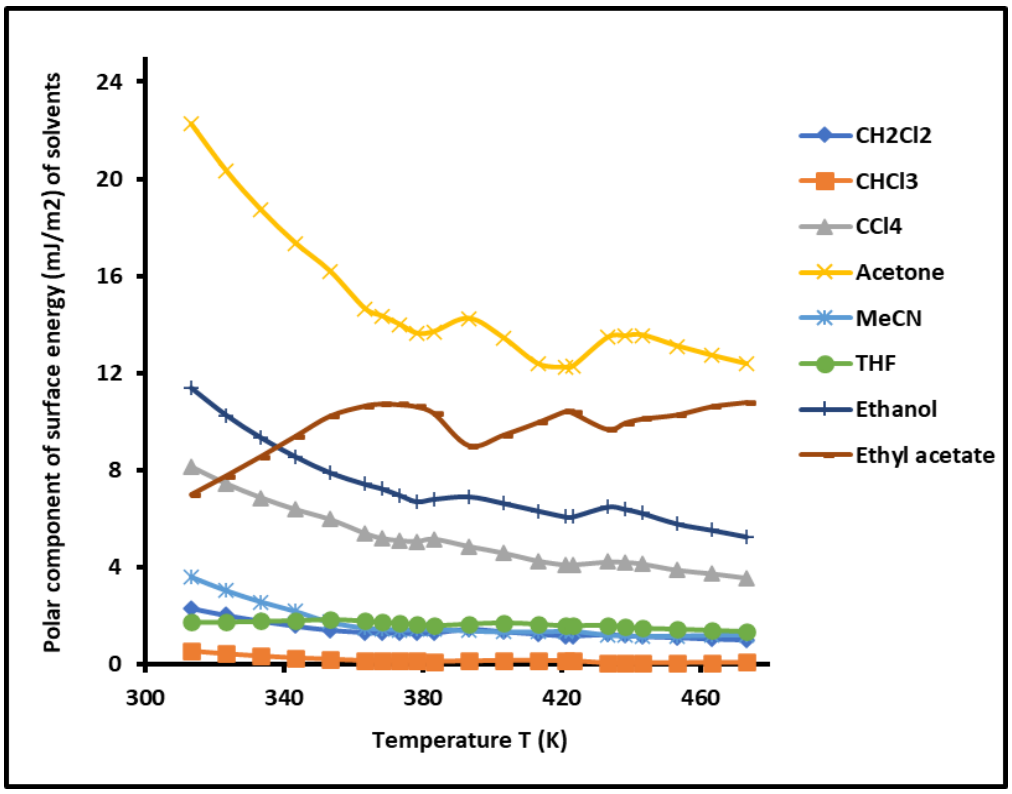

Figure 8. Variations of the polar component of the surface energy $\boldsymbol{\gamma_l^p(T)}$ (mJ/m²) of the different polar solvents adsorbed on the PS-*b*-P4VP diblock copolymer as a function of the temperature.

3.7. Work of Adhesion of Solvents on the PS-b-P4VP copolymer against the temperature

To determine the polar work of adhesion $W_a^p(Copolymer - X)$ of the polar organic molecule X adsorbed on the copolymer, the following relation was used: is given by relation 23:

$$W_a^p(Copolymer - X) = 2\sqrt{\gamma_s^p(Copolymer)\gamma_l^p(X)} \quad (23)$$

The variations of $W_a^p(Copolymer - X)$ versus the temperature were plotted in Figure 9. The plotted curves showed non-linear variations of the polar work of adhesion with the presence of two maxima at two particular temperatures corresponding to the two glass temperatures of the PS-*b*-P4VP diblock copolymer.

It was observed that the highest polar work of adhesion corresponded to the adhesion of acetone on the copolymer, followed by ethyl acetate, ethanol and CCl_4.

Preprints.org (www.preprints.org) | NOT PEER-REVIEWED | Posted: 17 September 2024 doi:10.20944/preprints202409.1337.v

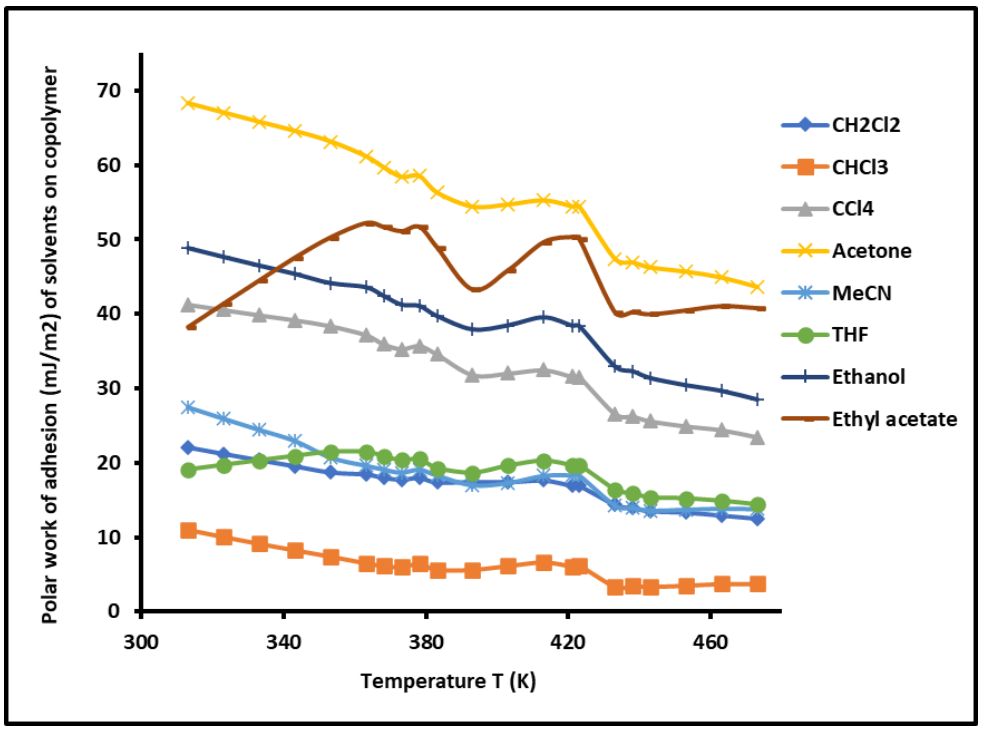

Figure 9. Evolution of $W_a^p(Copolymer - X)$ (mJ/m²) of polar molecules adsorbed on the PS-b-P4VP copolymer.

4. Conclusions

The surface thermodynamic properties of the PS-*b*-P4VP diblock copolymer were determined as a function of the temperature using the inverse gas chromatography technique at infinite dilution and applying the new methodology based on the Hamieh thermal model consisting in the accurate determination of the London dispersive surface energy of the copolymer, and on the London dispersion interaction equation allowing the separation between the Dispersive and polar free energies of adsorption of organic solvents on the PS-*b*-P4VP diblock copolymer. An important effect of the temperature on the Lewis's acid-base properties of the copolymer was showed. Two glass transition temperatures of the copolymer were highlighted, the first one at 105°C corresponding to the glass transition of PS polymer blocks and the second one at 148°C relative to that of P4VP blocks.

The variations of the free energy of adsorption, the London dispersive surface energy and the Lewis's acid and base surface energies of the copolymer as a function of the temperature all showed the presence of the two glass transition temperatures.

It was also showed that the variations of the different Lewis's acid-base parameters were non-linear with the presence of two maxima at the transition temperatures. An important basic character of the copolymer was observed and varying with the temperature. The calculations of the average values of the Lewis's acid-base parameters showed a copolymer surface 7.5 times more basic than acidic.

The separation distance between the organic molecules and the PS-*b*-P4VP diblock copolymer was determined and non-linear variations were also noticed with two minima observed at the glass transitions. An average value of the separation distance equal to 5.5Å was obtained. Our new methodology allowed obtaining the variations of the acid γ_s^+ and base γ_s^- surface energies, the polar acid-base surface energy γ_s^p, the London dispersive surface energy γ_s^d, and the Lifshitz – Van der Waals surface energy γ_s^{LW} (mJ/m²) of the PS-*b*-P4VP diblock copolymer as well as the polar surface energy of the solvents and their work of adhesion as a function of temperature.

Supplementary Materials: The following supporting information can be downloaded at: www.mdpi.com/xxx/s1, Table S1. Values of $RTlnVn$ (kJ/mol) of n-alkanes adsorbed on PS-P4VP copolymer as a function of temperature. Table S2. Values of $RTlnVn$ (kJ/mol) of polar solvents adsorbed on PS-P4VP copolymer

Preprints.org (www.preprints.org) | NOT PEER-REVIEWED | Posted: 17 September 2024 doi:10.20944/preprints202409.1337.v

as a function of temperature. Table S3. Values of $(-\Delta G_a^p(T)$ (kJ/mol) of polar solvents adsorbed on PS-P4VP copolymer as a function of temperature. Table S4. Values of $(-\Delta H_a^p(T)$ (kJ/mol) of polar solvents adsorbed on PS-P4VP copolymer as a function of temperature. Table S5. Values of $(-\Delta S_a^p(T)$ (J.mol^{-1}.K^{-1}) of polar solvents adsorbed on PS-P4VP copolymer as a function of temperature.

Funding: This research did not receive any specific grant.

Data Availability Statement: There is no additional data.

Conflicts of Interest: The author declares no conflict of interest.

References

1. Sunil, K.; Varshney, X.; Zhong, Y.; Eisenberg, A. Anionic homopolymerization and block copolymerization of 4-vinylpyridine and its investigation by high-temperature size exclusion chromatography in N-methyl-2-pyrrolidinone. *Macromolecules*, **1993**, *26*, 701-4. https://doi.org/10.1021/ma00056a022
2. Gao, Z.; Eisenberg, A. A. model of micellization for block copolymers in solutions. Macromolecules, **1993**, *26*, 7353-13. https://doi.org/10.1021/ma00078a035
3. Hong, K.; Urhig, D.; Mays, J.W. Living anionic polymerization, *Current Opinion in Solid State and Materials Science*, **1999**, *120*, 531-4. https://doi.org/10.1016/S1359-0286(00)00011-5
4. Ebdon, J.R.; Eastmond, G.C. New methods of polymer synthesis, Chap 2. Blackie Academic and Professional, Glasgow, UK, **1995**. https://doi.org/10.1007/978-94-011-0607-8
5. Huang, C.F.; Kuo, S.W.; Chen, J.K.; Chan, F.C. Synthesis and characterization of polystyrene-b-poly (4-vinyl pyridine) block copolymers by atom transfer radical polymerization. *Journal of Polymer Research*, **2005**, *12*, 449-6. https://doi.org/10.1007/s10965-004-5665-2
6. T.H. Kim, J. Huh, J. Hwang, H.-C. Kim, S.H. Kim, B.-H. Sohn, C. Park, Ordered arrays of PS-b-P4VP micelles by fusion and fission process upon solvent annealing, *Macromolecules*, **2009**, *42*, 6688–6697.
7. Hamley, I.W. Ordering in thin films of block copolymers: fundamentals to potential applications, *Prog. Polym. Sci*., 2009, 34, 1161–1210.
8. Wang, Y.; Narita, C.; Xu, X.; Honma, H.; Himeda, Y.; Yamada, K. Controlling the ordered transition of PS-b-P4VP block copolymer ultrathin films by solvent annealing, *Materials Chemistry and Physics*, **2020**, *239*, 122072, https://doi.org/10.1016/j.matchemphys.2019.122072
9. Hasegawa, H.; Hashimoto, T. Morphology of block copolymers and mixtures of block copolymers at free surfaces, *Polymer*, **1992**, *33*, 475-487.
10. Lee, D.H.; Cho, H.; Yoo, S.; Park, S. Ordering evolution of block copolymer thin films upon solvent-annealing process, *J. Colloid Interface Sci*., **2012**, *383*, 118-123.
11. Yan, N.; Wang Y. Reversible switch between the nanoporous and the nonporous state of amphiphilic block copolymer films regulated by selective swelling, *Soft Matter*, **2015**, *11*, 6927-6937.
12. Shamsudin, S.A.; Mikihito, T.; Hirokazu, H. Controlling ordered structures of PS-b-P2VP block copolymer thin film by tuning solvent evaporation rate, *Macromol. Symp*., **2017**, *371*,75-83.
13. Zha, W.; Han, C.D.; Lee, D.H.; Han, S.H.; Kim, J.K.; Kang, J.H.; Park, C. Origin of the difference in Order−Disorder transition temperature between polystyrene-block-poly(2-vinylpyridine) and polystyrene-block-poly(4-vinylpyridine) copolymers, *Macromolecules*, **2007**, 40, 2109-2119.
14. Yang, G.G.; Choi, H.J.; Han, K.H.; Kim, J.H.; Lee, C.W.; Jung, E.I.; *et al*. Block copolymer nanopatterning for non-semiconductor device applications, *ACS Appl Mater Inter*, **2022**, *14*, 12011-12037
15. Jeong, S.J.; Kim, J.Y.; Kim, B.H.; Moon, H.S.; Kim, S.O. Directed self-assembly of block copolymers for next generation nanolithography, *Mater Today*, **2013**, *16*, 468-476.
16. Angelopoulou, P.P.; Moutsios, I.; Manesi, G.M.; Ivanov, D.A.; Sakellariou, G.; Avgeropoulos, A. Designing high χ copolymer materials for nanotechnology applications: A systematic bulk vs. thin films approach, *Progress in Polymer Science*, **2022**, *135*, 101625, https://doi.org/10.1016/j.progpolymsci.2022.101625.
17. Cummins, C.; Pino, G.; Mantione, D.; Fleury, G. Engineering block copolymer materials for patterning ultra-low dimensions, *Mol Syst Des Eng*, **2020**, *5*, 1642-1657
18. Huang, C.F.; Kuo, S.W.; Chen, J.K., Chang, C.F. "Synthesis and Characterization of Polystyrene-b-Poly(4-vinyl pyridine) Block Copolymers by Atom Transfer Radical Polymerization." *Journal of Polymer Research*, **2015**, *12*, 449-456.
19. Guo, L.; Xia, D.; Wang, Y.; Ding, S.; Xu, J.; Zhu, Y.; Du, B. Fabrication of poly(4-vinylpyridine)-b-polystyrene-b-poly(4-vinylpyridine) triblock copolymer particles via three-dimensional soft confined self-assembly, *Polym. Chem.*, **2024**, *15*, 30-39.
20. Singh, S.; Ghoshal, T.; Prochukhan, N.; Fernandez, A.A.; Vasquez, J.F.B.; Yadav, P.; Padmanabhan, S.C.; Morris, M.A. Morphology Engineering of the Asymmetric PS-*b*-P4VP Block Copolymer: From Porous to Nanodot Oxide Structures, *ACS Applied Polymer Materials*, **2023**, *5* (11), 9612-9619, DOI: 10.1021/acsapm.3c02120

Preprints.org (www.preprints.org) | NOT PEER-REVIEWED | Posted: 17 September 2024 doi:10.20944/preprints202409.1337.v

21. Altug, H.; Oh, S.-H.; Maier, S. A.; Homola, J. Advances and Applications of Nanophotonic Biosensors. *Nat. Nanotechnol.* **2022**, *17* (1), 5– 16, DOI: 10.1038/s41565-021-01045-5
22. Krieg, L.; Meierhofer, F.; Gorny, S.; Leis, S.; Splith, D.; Zhang, Z.; von Wenckstern, H.; Grundmann, M.; Wang, X.; Hartmann, J.; et al. Toward Three-Dimensional Hybrid Inorganic/Organic Optoelectronics Based on GaN/OCVD-PEDOT Structures. *Nat. Commun.* **2020**, *11* (1), 5092, DOI: 10.1038/s41467-020-18914-7
23. Park, W.; Shin, H.; Choi, B.; Rhim, W.-K.; Na, K.; Keun Han, D. Advanced Hybrid Nanomaterials for Biomedical Applications. *Prog. Mater. Sci.* **2020**, *114*, 100686, DOI: 10.1016/j.pmatsci.2020.100686
24. Berman, D.; Shevchenko, E. Design of Functional Composite and All-Inorganic Nanostructured Materials *via* Infiltration of Polymer Templates with Inorganic Precursors. *J. Mater. Chem. C*, **2020**, *8* (31), 10604-10627, DOI: 10.1039/D0TC00483A
25. Singh, S.; Vasquez, J.F.B.; Perova, T.S.; Morris, M.A. Fabrication of metal-oxide arrays: mechanism of solvent-mediated metal infiltration into block copolymer nanopatterns. *Clean Techn Environ Policy*, **2023**, https://doi.org/10.1007/s10098-023-02678-x
26. Fang, X.; Bando, Y.; Gautam, U. K.; Ye, C.; Golberg, D. Inorganic Semiconductor Nanostructures and Their Field-Emission Applications. *J. Mater. Chem.* **2008**, *18* (5), 509– 522, DOI: 10.1039/B712874F
27. Diao, F.; Wang, Y. Transition Metal Oxide Nanostructures: Premeditated Fabrication and Applications in Electronic and Photonic Devices. *J. Mater. Sci.* **2018**, *53* (6), 4334– 4359, DOI: 10.1007/s10853-017-1862-3
28. Esmeraldo Paiva, A.; Baez Vasquez, J. F.; Selkirk, A.; Prochukhan, N.; Medeiros Borsagli, F. G. L.; Morris, M. Highly Ordered Porous Inorganic Structures *via* Block Copolymer Lithography: An Application of the Versatile and Selective Infiltration of the "Inverse" P2VP-*b*-PS System. *ACS Appl. Mater. Interfaces* **2022**, *14* (30), 35265– 35275, DOI: 10.1021/acsami.2c10338
29. Kang, D.-H.; Han, W. B.; Il Ryu, H.; Kim, N. H.; Kim, T. Y.; Choi, N.; Kang, J. Y.; Yu, Y. G.; Kim, T. S. Tunable and Scalable Fabrication of Block Copolymer-Based 3D Polymorphic Artificial Cell Membrane Array. *Nat. Commun.* **2022**, *13* (1), 1261, DOI: 10.1038/s41467-022-28960-y
30. Ghoshal, T.; Shaw, M. T.; Bolger, C. T.; Holmes, J. D.; Morris, M. A. A General Method for Controlled Nanopatterning of Oxide Dots: A Microphase Separated Block Copolymer Platform. *J. Mater. Chem.* **2012**, *22* (24), 12083, DOI: 10.1039/c2jm30468f
31. Bang, J.; Jeong, U.; Ryu, D. Y.; Russell, T. P.; Hawker, C. J. Block Copolymer Nanolithography: Translation of Molecular Level Control to Nanoscale Patterns. *Adv. Mater.* **2009**, *21* (47), 4769– 4792, DOI: 10.1002/adma.200803302
32. Bates, C. M.; Maher, M. J.; Janes, D. W.; Ellison, C. J.; Willson, C. G. Block Copolymer Lithography. *Macromolecules* **2014**, *47* (1), 2– 12, DOI: 10.1021/ma401762n
33. Kim, S. Y.; Gwyther, J.; Manners, I.; Chaikin, P. M.; Register, R. A. Metal-Containing Block Copolymer Thin Films Yield Wire Grid Polarizers with High Aspect Ratio. *Adv. Mater.* **2014**, *26* (5), 791– 795, DOI: 10.1002/adma.201303452
34. Ghoshal, T.; Prochukhan, N.; Morris, M. A. Sub-25 Nm Inorganic and Dielectric Nanopattern Arrays on Substrates: A Block Copolymer-Assisted Lithography. *ACS Omega* **2021**, *6* (51), 35738– 35744, DOI: 10.1021/acsomega.1c05124
35. Shevate, R.; Karunakaran, M.; Kumar, M.; Peinemann, K.-V. Polyanionic pH-responsive polystyrene-b-poly(4-vinyl pyridine-N-oxide) isoporous membranes, *Journal of Membrane Science*, **2016**, *501*, 161-168, https://doi.org/10.1016/j.memsci.2015.11.038.
36. Singh, S.; Horechyy, A.; Yadav, S.; Formanek, P.; Hübner, R.; Srivastava, R. K.; Sapra, S.; Fery, A.; Nandan, B. Nanoparticle Stabilized Perforated Lamellar Morphology in Block Copolymer /Quantum Dot, Hybrids, *Macromolecules*, **2021**, *54* (3), 1216– 1223, DOI:10.1021/acs.macromol.0c02639
37. Xue, F.; Li, H.; An, L.; Jiang, S. Constructional details of polystyrene-block-poly(4-vinylpyridine) ordered thin film morphology, *Journal of Colloid and Interface Science*, **2013**, *399*, 62-67,https://doi.org/10.1016/j.jcis.2013.02.033
38. Schulze, M.; Handge, U.A.; Rangou, S.; Lillepärg, J.; Abetz, V. Thermal properties, rheology and foams of polystyrene-block-poly(4-vinylpyridine) diblock copolymers, *Polymer*, **2015**, *70*, 88-99, https://doi.org/10.1016/j.polymer.2015.06.005.
39. Zhang, B.-Q.; Chen, G.-D.; Pan, C.-Y.; Luan, B.; Hong, C.-Y. Preparation, characterization, and thermal properties of polystyrene-*block*-quaternized poly(4-vinylpyridine)/Montmorillonite nanocomposites. *J. Appl. Polym. Sci.*, **2006**, *102*, 1950-1958. https://doi.org/10.1002/app.24491.
40. Conder, J. R.; Young, C. L. Physical measurements by gas chromatography. Eds: John Wiley & Sons, Chichester, New York, 1979, 632 pages.
41. Sawyer, D.T.; Brookman, D.J. Thermodynamically based gas chromatographic retention index for organic molecules using salt-modified aluminas and porous silica beads, *Anal. Chem.* **1968**, *40*, 1847-1850. https://doi.org/10.1021/ac60268a015.
42. Dorris, G.M.; Gray, D.G. Adsorption of n-alkanes at zero surface coverage on cellulose paper and wood fibers, *J. Colloid Interface Sci.* **1980**, *77*, 353-362.

Preprints.org (www.preprints.org) | NOT PEER-REVIEWED | Posted: 17 September 2024 doi:10.20944/preprints202409.1337.v

43. Fowkes, F.M. in: Surface and interfacial aspects of biomedical polymers, Vol. I, pp. 337-372, Ed: J. D. Andrade, Plenum Press, New York, 1985.
44. Schultz, J.; Lavielle, L.; Martin, C. The role of the interface in carbon fibre-epoxy composites. *J. Adhes.* **1987**, *23*, 45-60.
45. Saint-Flour, C.; Papirer, E. Gas-solid chromatography. A method of measuring surface free energy characteristics of short glass fibers. 1. Through adsorption isotherms, *Ind. Eng. Chem. Prod. Res. Dev.* **1982**, 21, 337-341, https://doi.org/10.1021/i300006a029
46. Saint-Flour, C.; Papirer, E. Gas-solid chromatography: method of measuring surface free energy characteristics of short fibers. 2. Through retention volumes measured near zero surface coverage, *Ind. Eng. Chem. Prod. Res. Dev.* **1982**, 21, 666-669, https://doi.org/10.1021/i300008a031
47. Donnet, J.-B.; Park, S.; Balard, H. Evaluation of specific interactions of solid surfaces by inverse gas chromatography, *Chromatographia*. **1991**, *31*, 434–440.
48. Brendlé, E.; Papirer, E. A new topological index for molecular probes used in inverse gas chromatography for the surface nanorugosity evaluation, 1. Method of Evaluation, *J. Colloid Interface Sci.* **1997**, *194*, 207–216.
49. Brendlé, E.; Papirer, E. A new topological index for molecular probes used in inverse gas chromatography for the surface nanorugosity evaluation, 2. Application for the Evaluation of the Solid Surface Specific Interaction Potential, *J. Colloid Interface Sci*. **1997**, *194*, 217–2224.
50. Hamieh, T.; Schultz, J. New approach to characterize physicochemical properties of solid substrates by inverse gas chromatography at infinite dilution. Some new methods to determine the surface areas of some molecules adsorbed on solid surfaces. *J. Chromatogr. A* **2002**, *969*, 17–47. https://doi.org/10.1016/S0021-9673(02)00368-0.
51. Voelkel, A. Inverse gas chromatography: Characterization of polymers, fibers, modified silicas, and surfactants. *Crit. Rev. Anal. Chem.* **1991**, *22*, 411–439. https://doi.org/10.1080/10408349108051641.
52. Papadopoulou, S.K.; Panayiotou, C. Assessment of the thermodynamic properties of poly(2,2,2-trifluoroethyl methacrylate) by inverse gas chromatography, *J. Chromatogr. A*, **2014**, 1324, 207– 214. https://doi.org/10.1016/j.chroma.2013.11.044.
53. Hamieh, T. Study of the temperature effect on the surface area of model organic molecules, the dispersive surface energy and the surface properties of solids by inverse gas chromatography. *J. Chromatogr. A* **2020**, *1627*, 461372.
54. Hamieh, T. New methodology to study the dispersive component of the surface energy and acid–base properties of silica particles by inverse gas chromatography at infinite dilution. *J. Chromatogr. Sci.* **2022**, *60*, 126–142. https://doi.org/10.1093/chromsci/bmab066.
55. Hamieh, T.; Ahmad, A.A.; Roques-Carmes, T.; Toufaily, J. New approach to determine the surface and interface thermodynamic properties of H-β-zeolite/rhodium catalysts by inverse gas chromatography at infinite dilution. *Sci. Rep.* **2020**, *10*, 20894. https://doi.org/10.1038/s41598-020-78071-1.
56. Hamieh, T. Some Irregularities in the Evaluation of Surface Parameters of Solid Materials by Inverse Gas Chromatography, *Langmuir* **2023** *39, 17059-17070,* https://doi.org/10.1021/acs.langmuir.3c01649.
57. Hamieh, T. New physicochemical methodology for the determination of the surface thermodynamic properties of solid particles. *Appl. Chem.* **2023**, *3*, 229–255. https://doi.org/10.3390/appliedchem3020015.
58. Hamieh, T. New Progress on London Dispersive Energy, Polar Surface Interactions, and Lewis's Acid–Base Properties of Solid Surfaces. *Molecules* **2024**, *29*, 949. https://doi.org/10.3390/molecules29050949.
59. Hamieh, T. London Dispersive and Lewis Acid-Base Surface Energy of 2D Single-Crystalline and Polycrystalline Covalent Organic Frameworks. *Crystals* **2024**, *14*, 148. https://doi.org/10.3390/cryst14020148.
60. Hamieh, T. Inverse Gas Chromatography to Characterize the Surface Properties of Solid Materials. *Chem. Mater.* **2024**, *36*, 2231–2244. https://doi.org/10.1021/acs.chemmater.3c03091.
61. Hamieh, T. Effect of Tacticity on London Dispersive Surface Energy, Polar Free Energy and Lewis Acid-Base Surface Energies of Poly Methyl Methacrylate by Inverse Gas Chromatography. *Macromol* **2024**, *4*, 356-375. https://doi.org/10.3390/macromol4020020.
62. Hamieh, T. The Effect of Temperature on the London Dispersive and Lewis Acid-Base Surface Energies of Polymethyl Methacrylate Adsorbed on Silica by Inverse Gas Chromatography. *Thermo* **2024**, *4*, 202-221. https://doi.org/10.3390/thermo4020012.
63. Hamieh, T. Temperature Dependence of the Polar and Lewis Acid–Base Properties of Poly Methyl Methacrylate Adsorbed on Silica via Inverse Gas Chromatography. *Molecules* **2024**, *29*, 1688. https://doi.org/10.3390/molecules29081688
64. Rajab, M.; Hamieh, T.; Airoudj, A.; Mougin, K.; Hariri, K.; Rammal, W.; Mortada, H.; Akil, M.; Kassas, A.; Toufaily, J. Synthesis by ATRP of Polystyrene-b-Poly(4-vinylpyridine) and Characterization by Inverse Gas Chromatography. *Journal of Research Updates in Polymer Science*, **2017**, *6*(3), 76–89. https://doi.org/10.6000/1929-5995.2017.06.03.2
65. G.M. Dorris, D.G. Gray, Adsorption of n-alkanes at zero surface coverage on cellulose paper and wood fibers, J. Colloid Interface Sci., 77 (1980) 353–362

Preprints.org (www.preprints.org) | NOT PEER-REVIEWED | Posted: 17 September 2024 doi:10.20944/preprints202409.1337.v

66. F.M. Fowkes, in: Surface and interfacial aspects of biomedical polymers, Vol. I, pp. 337-372, Ed: J. D. Andrade, Plenum Press, New York (1985).
67. Gutmann, V. The Donor-Acceptor Approach to Molecular Interactions; Plenum: New York, NY, USA, 1978.
68. Riddle, F.L.; Fowkes, F.M. Spectral shifts in acid-base chemistry. Van der Waals contributions to acceptor numbers, Spectral shifts in acid-base chemistry. 1. van der Waals contributions to acceptor numbers. *J. Am. Chem. Soc.* **1990**, *112*, 3259–3264. https://doi.org/10.1021/ja00165a001.
69. C.J. Van Oss, R.J. Good, M.K. Chaudhury, Additive and nonadditive surface tension components and the interpretation of contact angles, Langmuir, 1988, 4 (4) 884, http:// dx.doi.org/10.1021/la00082a018.
70. Zhang, B.-Q.; Chen, G.-D.; Pan, C.-Y.; Luan, B.; Hong, C.-Y. Preparation, Characterization, and Thermal Properties of Polystyrene-block-Quaternized Poly(4 vinylpyridine)/Montmorillonite Nanocomposites, *Journal of Applied Polymer Science*, **2006**, *102*, 1950–1958. **https://doi.org/10.1002/app.24491.**
71. Zhao, J., Tian, S., Wang, Q.; Xiaobo Liu, X.; Jiang, S.; Ji, X.; An, L.; Jiang, B. Nanoscopic surface patterns of diblock copolymer thin films. *Eur. Phys. J. E* **16**, 49–56 (2005). https://doi.org/10.1140/epje/e2005-00006-1
72. Saleem, S.; Rangou, S.; Abetz, C.; Filiz, V.; Abetz, V. Isoporous Membranes from Novel Polystyrene-*b*-poly(4-vinylpyridine)-*b*-poly(solketal methacrylate) (PS-*b*-P4VP-*b*-PSMA) Triblock Terpolymers and Their Post-Modification. *Polymers* **2020**, *12*, 41. https://doi.org/10.3390/polym12010041
73. Xue, F.; Li, H.; An, L.; Jiang, S. Constructional details of polystyrene-block-poly(4-vinylpyridine) ordered thin film morphology, *Journal of Colloid and Interface Science*, **2013**, *399*, 62-67, https://doi.org/10.1016/j.jcis.2013.02.033
74. A. Rahikkala, A.; Soininen, A.; Ruokolainen, J.; Mezzenga, R.; Raula, J.; Kauppinen, E. Self-assembly of PS-b-P4VP block copolymers of varying architectures in aerosol nanospheres. *Soft Matter*, 2013, 9, 1492-1499. https://doi.org/10.1039/C2SM26913A
75. Huang, C.-F.; Kuo, S.-W.; Chen, J.K.; Chang, F.C. Synthesis and Characterization of Polystyrene-*b*-Poly(4-vinyl pyridine) Block Copolymers by Atom Transfer Radical Polymerization, Journal of Polymer Research, **2005**, *12*, 449–456, https://doi.org/10.1007/s10965-004-5665-2.
76. David, R.L. (Ed.) *CRC Handbook of Chemistry and Physics, Internet Version 2007*, 87th ed.; Taylor and Francis: Boca Raton, FL, USA, 2007. http:/www.hbcpnetbase.com (accessed on 1 May 2024).
77. Hamieh, T. Surface Thermodynamic Properties of Poly Lactic Acid by Inverse Gas Chromatography. *Biomimetics* **2024**, *9*, 268. https://doi.org/10.3390/biomimetics9050268.

Disclaimer/Publisher's Note: The statements, opinions and data contained in all publications are solely those of the individual author(s) and contributor(s) and not of MDPI and/or the editor(s). MDPI and/or the editor(s) disclaim responsibility for any injury to people or property resulting from any ideas, methods, instructions or products referred to in the content.